Analysis of Model of Soil Freezing and Thawing

Alexandr Žák, Michal Beneš, and Tissa H. Illangasekare

Abstract—**The article studies a time dependent mathematical model of two-dimensional two-phase system describing a cross-section of saturated soil sample in terms of its temperature. The model is used to control the structural conditions in the medium by coupling it with the Navier equations. The computational studies of this coupling are presented at the end of the article. The thermal model setting and its variational formulation are presented as well as a basic analysis of mathematical properties of the partial problem solution.**

Index Terms—**analysis, freezing, model, phase-change, soil**

I. Introduction

SOIL is a common material covering the land surface. It plays a significant role, among others, in civil engineering when designing structures. From the engineering viewpoint, the term soil can be understood as a porous, basically loose, material whose solid constituent consists of rock particles (grains) and whose pores are usually filled with water (saturated soil) or water and gases (unsaturated soil). Physical properties of soil vary depending on the size and the material of the grains, on the proportional representation of the sizes and the materials in a given volume, on the amount of the pore water (saturation), on the neighbouring geological conditions, and the climate. As these parameters change in time, the physical properties may gradually change as well. In consequence of the interaction of soil surface and environs, the deformations of the ground surface may appear in the course of time. As the structure or building foundations are (mechanically) affected by great mass of soil material, even a relatively small change of the soil properties can have a considerable impact.

One of the processes leading to the considerable changes of the soil layers properties is the frost heave. It occurs in the cold regions of the Earth where the soil with the specific range of soil grain sizes and the sufficient amount of the pore water can be found. The frost heave causes upward displacement of the top ground layer when the ground temperature decreases below the freezing point of water. The principal cause of the frost heave was ascribed to the formation of ice lenses by Taber in 1929 ([1]). The ice formation takes place at the freezing front due to the discontinuity in heat flux or a short distance above the front due to the regelation mechanism. Referring to the dependence on one of the forming mechanisms, the terms primary and secondary heaving, respectively, are used. The ice lens growth is caused by a suction of water from below to the lens basal surface, where it freezes.

The secondary heaving mechanism is more important in general, as it heaves larger loads, and was described by Miller in 1978 ([2]). After that, some prediction models of frost heave rate and ice lensing have followed considering the thermomechanical processes at the microscopic level and aiming at fundamental understanding of the phenomena (e.g., Gilpin 1980, [3], O'Neil and Miller 1985, [4], Fowler 1989, [5]). An opposite (macroscopic) approach to the frost heave modeling can be found in the constitutive models using the definition of frost susceptibility as the property of soil and focusing on quantitative and qualitative prediction of frost heave (e.g., Michalowski 1993, [6], Michalowski and Zhu 2005, [7]). Some models describing partial aspects related to the frost heave mechanism have been separately developed as well. For example, the model for coupled water flow and heat transport ([8]), the model for solidification of porous material under natural convection ([9]), or the models concerning fluid flow in porous media (e.g. [11], [10], [12]). Only lately, the first more comprehensive models based on thermodynamics and coupling more physical quantities have been presented. They include the soil freezing model by Mikkola and Hartikainen (1997 [13], 2001 [14]), which incorporates some parameters without physical meaning, the basic modeling framework for freezing soil by Li et al. (2002 [15], 2008 [16]), and the poroelastic modeling framework of freezing materials by Coussy (2005 [17]), which was further generalized by Aichi and Tokunaga (2012 [18]). It can be noticed that the so far developed soil freezing models mostly do not consider the inverse process of soil thawing and that the respective computational studies are usually oriented to the freezing scenario only.

Currently, many regions of the globe face the observable climate change. It includes shifts in seasonal temperatures, costal erosion, increased storm effects, sea ice retreat, and permafrost thawing. In cold regions, especially in those areas where permafrost currently or in the future may be subjected to excessive thawing, serious risks of changes in mechanical behaviour of upper soil layers arise. The climate change introduces uncertainty and variability into the design of future infrastructures and into the operation and maintenance of infrastructures already placed there. Thus, it is desirable to improve knowledge of the effect of permafrost thawing on foundations, roads, and runways or the effect of the thermal profile of structures and the adjacent land use on soil freeze-thaw cycling.

In an effort to contribute to better understanding of the impacts of climate change on mechanical behaviour of soil surface, a two-dimensional thermomechanical model of a

Manuscript received September 26, 2012; revised July 22, 2013. Partial support of the project of the "Numerical Methods for Multi-phase Flow and Transport in Subsurface Environmental Applications, project of Czech Ministry of Education, Youth and Sports Kontakt ME10009, 2010-2012" and of the project "Advanced Supercomputing Methods for Implementation of Mathematical Models, project of the Student Grant Agency of the Czech Technical University in Prague No. SGS11/161/OHK4/3T/14, 2011-13".

A. Žák and M. Beneš are with the Department of Mathematics, Faculty of Nuclear Sciences and Physical Engineering, Czech Technical University in Prague, e-mail: alexandr.zak@fjfi.cvut.cz (corresponding author), michal.benes@fjfi.cvut.cz, respectively.

T. H. Illangasekare is with the Center for Experimental Study of Subsurface Environmental Processes, Colorado School of Mines, e-mail: tissa@mines.edu.

soil layer profile is introduced in this paper. The model is based on continuum approach. It considers the heat and momentum balance relations and adopts an empirical linking term. Thus, it allows to obtain the computational studies of the subsurface thawing and freezing layers. The model is supposed to be the first step towards the design of a comprehensive soil freezing and thawing model which would be as computationally undemanding as possible and, at the same time, still sufficiently accurate.

II. Mathematical model

The proposed model serves for the description of a two-dimensional soil profile and, in contrast to, e.g., [13], [16], [17], views soil as an elementary continuum material. The soil material is assumed to be continuously and uniformly spread out over the occupied space and is characterized at each point of the space by the temperature and by the displacement vector.

To express the heat transport in the studied soil, the modified heat equation for the soil temperature $u = u(t, \mathbf{x})$ (in °C), which describes the phase change in a neighborhood of the freezing point depression $u^\star$ (temperature at which pore water freezes and which is slightly lower than the freezing point of pure water), $u^\star < 0$, is considered. The equation has the form

$$C\frac{\partial}{\partial t}u + L\frac{\partial}{\partial t}\theta(u) = \lambda\Delta u\,, \tag{1}$$

where C, L, λ are the volumetric heat capacity, the volumetric latent heat of freezing of water, and thermal conductivity, respectively. Using approach taken from [19], the volumetric unfrozen water content is described by the power function θ,

$$\theta(u) = \eta\phi(u)\,, \quad \phi(u) = \begin{cases} 1 & : \quad u \geq u^\star \\ \left|\frac{u^\star}{u}\right|^b & : \quad u < u^\star \end{cases}\,,$$

where η is the soil porosity of melt-state soil, ϕ represents the liquid pore water fraction, and b is a positive constant related to the material characteristic of the soil.

When interested in the deformation effects of the freezing and thawing on saturated soil, the momentum conservation is considered. With regard to the fact that the deformation is caused by the inner stress change in the material induced by the water-ice phase transition of the water fraction, a stress switch function can be used to couple the temperature and the displacement vector. Motivated by the empirical knowledge that freezing water in a fixed volume increases abruptly the inner stress, the function can be written in the form of the step function

$$\xi(u) = \chi\vartheta(u^\star - u)\,, \tag{2}$$

where χ is internal stress rate expressing the jump in stress during the cooling the material below $u^\star$ and where ϑ denotes the Heaviside step function. Then, the appropriate scaling of χ can incorporate the stress increase resulting from the water density change during the water-ice transition and the average effect of the lens formation as well. Thus, assuming the stress change induced by (2), the Navier equations for the displacement vector (v, w) are as follows

$$\varrho\frac{\partial^2}{\partial t^2}\begin{bmatrix} v \\ w \end{bmatrix} + \nabla\cdot\Gamma = 0\,, \tag{3}$$

where ϱ is the soil density, Γ stands for

$$\begin{bmatrix} E\dfrac{(\nu-1)\frac{\partial}{\partial x}v - \nu\frac{\partial}{\partial y}w}{(1+\nu)(1-2\nu)} + \xi\,, & \dfrac{-E}{2(1+\nu)}\left(\frac{\partial}{\partial y}v + \frac{\partial}{\partial x}w\right) \\ \dfrac{-E}{2(1+\nu)}\left(\frac{\partial}{\partial y}v + \frac{\partial}{\partial x}w\right)\,, & E\dfrac{-\nu\frac{\partial}{\partial x}v + (\nu-1)\frac{\partial}{\partial y}w}{(1+\nu)(1-2\nu)} + \xi \end{bmatrix}\,,$$

E is Young's modulus, and ν is Poisson's ratio.

The model governed by (1) and (3) and supplemented by the suitable boundary and initial conditions serves as a simple phase and structure change model. This model can be solved numerically. Corresponding computational studies are presented in Section V. They provide a qualitative information on the soil freezing and thawing processes in a vertical 2D cut.

III. Analysis

The model (1), (3) can become subject of mathematical interest as well. In particular, energy equation (1) controlling the phase change process is discussed in detail here.

Let Ω be the rectangular domain $]0, x_1[\times]z_1, 0[$ and Q denote $]0, T[\times\Omega$ for some $T > 0$. The problem given by equation (1) is considered as follows

$$C\frac{\partial}{\partial t}u(t,\mathbf{x}) + L\frac{\partial}{\partial t}\theta(u(t,\mathbf{x})) = \lambda\Delta u(t,\mathbf{x})\,, \quad (t,\mathbf{x}) \in Q\,,$$

where C, L, and λ are, for simplicity, constants. Further, the equation is supplemented by the initial temperature distribution

$$u(0,\mathbf{x}) = u_0(\mathbf{x})\,, \quad \mathbf{x} \in \bar{\Omega}\,, \tag{4}$$

and by the homogeneous Dirichlet boundary conditions

$$u(t,\mathbf{x}) = 0\,, \quad \mathbf{x} \in \partial\Omega\,,\ t \in]0, T[\,. \tag{5}$$

Considering the model settings, it is possible to find an analogy between this problem and the Stefan problem ([20], [21], [22]).

A. Enthalpy formulation

For the purpose of the mathematical analysis, it is proceeded to an enthalpy formulation of equation (1)

$$\frac{\partial}{\partial t}H(u) = \lambda\Delta u\,, \tag{6}$$

which can be obtained by the substitution

$$H(u) = \int_{u_{min}}^{u} C\,\mathrm{d}\xi + L\theta(u)$$

on the left-hand side (u_{min} is a constant value). Note that H is continuous and its first derivative is continuous everywhere except for $u^\star$. The value $u^\star$ becomes a singularity in equation (1) or (6).

B. Variational formulation

Equation (6) is multiplied by a test function v from $\mathcal{C}^2(Q) \cap \mathcal{C}^1(\bar{Q})$ vanishing for all $\mathbf{x} \in \partial\Omega$, $t \in [0, T]$ and

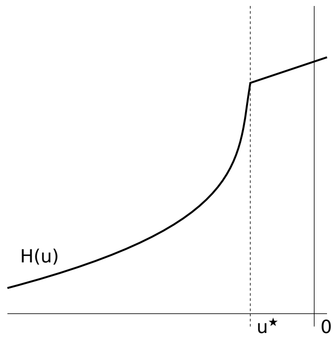

Fig. 1. Illustration of the function H.

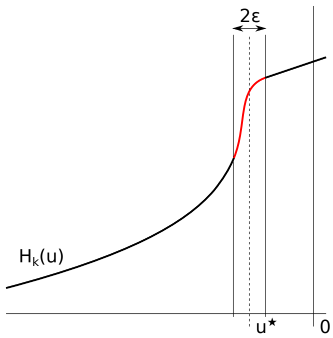

Fig. 2. Illustration of the function H_k.

for all $\mathbf{x} \in \bar{\Omega}$, $t = T$ and integrated over Q. Using the Green formula, it can be gradually treated:

$$0 = \int_Q \left(\frac{\partial}{\partial t} H(u)v - \lambda \Delta u v \right) \mathrm{d}\mathbf{x}\mathrm{d}t \,,$$

$$0 = \int_Q \left(\frac{\partial}{\partial t} H(u)v + \lambda \nabla u \nabla v \right) \mathrm{d}\mathbf{x}\mathrm{d}t - \lambda \int_0^T \int_{\partial\Omega} \nabla u \vec{n} v \, \mathrm{d}s\mathrm{d}t \,,$$

$$0 = \left[\int_\Omega H(u)v \, \mathrm{d}\mathbf{x} \right]_0^T - \int_Q \left(H(u) \frac{\partial}{\partial t} v - \lambda \nabla u \nabla v \right) \mathrm{d}\mathbf{x}\mathrm{d}t \,,$$

$$0 = \int_Q \left(H(u) \frac{\partial}{\partial t} v - \lambda \nabla u \nabla v \right) \mathrm{d}\mathbf{x}\mathrm{d}t + \int_\Omega H(u_0(\mathbf{x}))v(0,\mathbf{x}) \, \mathrm{d}\mathbf{x} \,. \tag{7}$$

It is now possible to define the weak solution.

Definition III.1. *The weak solution of problem (6) with (4) and (5) is the function $u \in H^1(Q)$ which satisfies relation (5) in the sense of traces and (7) for all test functions $v \in \mathcal{C}^2(Q) \cap \mathcal{C}^1(\bar{Q})$, $v = 0$ for $\forall \mathbf{x} \in \partial\Omega$, $t \in [0,T]$ and for $\forall \mathbf{x} \in \bar{\Omega}$, $t = T$.*

Remark III.1. *It is obvious that each classical solution of problem (6) with (4), (5) is the weak solution.*

C. Uniqueness of solution

Theorem III.1. *The weak solution of the problem (6) with (4), (5) is unique.*

Proof: Let there exist two different solutions u_1 and u_2 of the problem. Inserting them into equation (7) and subtracting these equations, it follows

$$\int_Q \Big([H(u_1) - H(u_2)] \frac{\partial}{\partial t} v - \lambda [\nabla u_1 - \nabla u_2] \nabla v \Big) \mathrm{d}\mathbf{x}\mathrm{d}t = 0 \,.$$

The Green formula yields

$$\int_Q \left([H(u_1) - H(u_2)] \frac{\partial}{\partial t} v + \lambda [u_1 - u_2] \Delta v \right) \mathrm{d}\mathbf{x}\mathrm{d}t = 0 \,.$$

The equation is further rewritten as

$$\int_Q \left([H(u_1) - H(u_2)] \times \left[\frac{\partial}{\partial t} v + \lambda \frac{u_1 - u_2}{H(u_1) - H(u_2)} \Delta v \right] \right) \mathrm{d}\mathbf{x}\mathrm{d}t = 0 \,.$$

Now, the following lemma, which is referred to in [23] (and which can be verified for this case), can be used.

Lemma III.1.

$$\int_Q [H(u_1) - H(u_2)] \, \phi \, \mathrm{d}\mathbf{x}\mathrm{d}t = 0$$

holds for all $\phi \in \mathcal{C}^\infty(Q)$ with $\mathrm{supp}\phi \subset Q$.

Thus, considering the fact that a set of such functions ϕ is dense in $L^2(Q)$, it can be concluded that $H(u_1) = H(u_2)$ almost everywhere on Q and, since H is monotone, also that $u_1 = u_2$. ■

Remark III.2. *Remark III.1 implies that the classical solution is unique as well.*

IV. Existence of solution

Since the function H has convenient properties for the purpose of analysis except the behavior at the point $u^\star$, the existence of a solution is investigated by regularization. The sequence of problems with mollified functions H_k, whose first derivative is continuous everywhere and whose limit is the function H, is constructed. The regularized functions can be gradually constructed by substitution of the original function H on some interval for a part of a smooth function when, simultaneously, the length of superseded interval tends to zero as the sequence index increases. For specific choice of functions H_k sequence, it can be referred to, e.g., [24].

Thus, the following sequence of problems is considered

$$\frac{\partial}{\partial t} H_k(u) = \lambda \Delta u \,,$$
$$u(0) = u_0 \,,$$
$$u|_{\partial\Omega} = 0 \,,$$

where $k \in \mathbb{N}$ and $H_k \to H$ as $k \to \infty$. The solution of the problem with H_k is denoted as u^k; the limit of $\{u^k\}_{n \in \mathbb{N}}$ will be studied. Next, the existence of their solutions is investigated.

A. Galerkin method

The solution existence of an arbitrary (k is now fixed) smoothed problem can be shown by means of the Galerkin approximation. Let V_n, $n \in \mathbb{N}$, be the finite dimensional subspace of $L^2(Q)$ generated by the first n (normed) eigenvectors, $v_1, \ldots, v_n$, of the Laplace operator on Ω coupled with the homogeneous Dirichlet boundary conditions, and let

$(.,.)$ denote the scalar product on $L^2(\Omega)$. The solution u_n^k from $[0,T[$ to V_n of an auxiliary problem is sought using the variational formulation in the space,

$$0 = \left(\frac{\partial}{\partial t} H_k(u_n^k), v\right) + \lambda\left(\nabla u_n^k, \nabla v\right)\,, \quad \forall v \in V_n\,, \qquad u_n^k(0) = \mathcal{P}_n u_0\,, \tag{8}$$

where $\mathcal{P}_n : L^2(Q) \to V_n$ is the projection operator.

1) System of ODE's: The solution of (8) is expressed as the linear combination of the basis functions of V_n

$$u_n^k(t) = \sum_{i=1}^{n} a_i^k(t) v_i\,,$$

where a_i^k, $i \in \{1,\ldots,n\}$, are the unknown time-dependent coefficients. Equation (8) is tested by v_j, $j \in \{1,\ldots,n\}$ to obtain a system of differential equations for the coefficients beta. Then for arbitrary j, it follows

$$\begin{aligned} 0 &= \left(\frac{\partial}{\partial t} H_k(u_n^k), v_j\right) + \lambda\left(\nabla u_n^k, \nabla v_j\right)\,, \\ 0 &= \sum_{i=1}^{n} \frac{\partial}{\partial t} a_i^k \left(H_k'(u_n^k) v_i, v_j\right) - \lambda \sum_{i=1}^{n} \beta_i a_i^k \left(v_i, v_j\right)\,, \\ 0 &= \sum_{i=1}^{n} \frac{\partial}{\partial t} a_i^k \left(H_k'(u_n^k) v_i, v_j\right) - \lambda \beta_j a_j^k\,, \end{aligned} \tag{9}$$

where β_i are the corresponding eigenvalues of the operator. Denoting $\mathbf{a}^k = (a_1^k,\ldots,a_n^k)$, time derivative of $\mathbf{a}^k$ by $\dot{\mathbf{a}}^k$, $\Lambda = \mathrm{diag}\{\beta_1,\ldots,\beta_n\}$, and $\mathbb{M}_{ij}^k = \mathbb{M}_{ij}^k(\mathbf{a}^k) = \left(H_k'(u_n^k)v_i, v_j\right)$, the required system of (9), where $j \in \{1,\ldots,n\}$, can be written as

$$\mathbb{M}^k(\mathbf{a}^k)\dot{\mathbf{a}}^k - \lambda\Lambda\mathbf{a}^k = 0\,. \tag{10}$$

System (10) is a system of ODE's. For arbitrary $h \in \mathbb{R}^n - \{0\}$, it is observed that

$$\begin{aligned} h\mathbb{M}^k h &= \sum_{i,j=1}^{n} \mathbb{M}_{ij}^k h_i h_j = \sum_{i,j=1}^{n} \left(H_k' v_i, v_j\right) h_i h_j \\ &= \left(H_k' \sum_{i=1}^{n} h_i v_i, \sum_{j=1}^{n} h_j v_j\right) = \left(H_k'\varphi, \varphi\right) \\ &\geq c_0 \|\varphi\|_{L^2(\Omega)}^2 > 0\,, \end{aligned}$$

which implies that $\mathbb{M}^k$ is positive-definite for all $\mathbf{a}^k$. Therefore, there always exists the inverse matrix to $\mathbb{M}^k$. Then, (10) can be converted into the normal system, and the usual existence theory of ODE's can be applied.

2) A priori estimates: Estimates for investigation of the convergence of $\{u_n^k\}_{n\in\mathbb{N}}$ will be derived. Equation (8) is tested by $\frac{\partial}{\partial t} u_n^k$, which implies that

$$\begin{aligned} 0 &= \left(H_k'(u_n^k)\frac{\partial}{\partial t} u_n^k, \frac{\partial}{\partial t} u_n^k\right) + \lambda\left(\nabla u_n^k, \nabla \frac{\partial}{\partial t} u_n^k\right)\,, \\ 0 &= \left(H_k'(u_n^k)\frac{\partial}{\partial t} u_n^k, \frac{\partial}{\partial t} u_n^k\right) + \frac{1}{2}\lambda \frac{\mathrm{d}}{\mathrm{d}t}\left\|\nabla u_n^k\right\|_{L^2(\Omega)}^2\,, \\ 0 &\geq c_0 \left\|\frac{\partial}{\partial t} u_n^k\right\|_{L^2(\Omega)}^2 + \frac{1}{2}\lambda \frac{\mathrm{d}}{\mathrm{d}t}\left\|\nabla u_n^k\right\|_{L^2(\Omega)}^2\,, \qquad (11) \\ 0 &\geq \frac{\mathrm{d}}{\mathrm{d}t}\left\|\nabla u_n^k\right\|_{L^2(\Omega)}^2\,. \end{aligned}$$

The last inequality is integrated over $[0,\tau]$, $\tau \leq T$; it follows

$$\begin{aligned} \left\|\nabla u_n^k(\tau)\right\|_{L^2(\Omega)}^2 &\leq \left\|\nabla u_n^k(0)\right\|_{L^2(\Omega)}^2 \\ &= \left\|\nabla \mathcal{P}_n u_0\right\|_{L^2(\Omega)}^2 \leq \left\|\nabla u_0\right\|_{L^2(\Omega)}^2 \\ &\leq |\Omega| c_1(u_0)\,, \end{aligned} \tag{12}$$

where the constant c_1 depends on the initial function u_0 and $|\Omega|$ denotes the Lebesgue measure of the domain Ω. The Poincaré inequality is used to obtain the lower bound. Then, together, it yields

$$\frac{1}{c_2(\Omega)}\left\|u_n^k(\tau)\right\|_{L^2(\Omega)}^2 \leq \left\|\nabla u_n^k(\tau)\right\|_{L^2(\Omega)}^2 \leq |\Omega| c_1(u_0)\,, \tag{13}$$

where c_2 is the Poincaré constant. Further, from (11), it follows

$$\begin{aligned} c_0 \left\|\frac{\partial}{\partial t} u_n^k(\tau)\right\|_{L^2(Q)}^2 &+ \frac{\lambda}{2}\left\|\nabla u_n^k(T)\right\|_{L^2(\Omega)}^2 \\ &- \frac{\lambda}{2}\left\|\nabla u_n^k(0)\right\|_{L^2(\Omega)}^2 \leq 0 \end{aligned}$$

and then

$$\begin{aligned} c_0' \left\|\frac{\partial}{\partial t} u_n^k(\tau)\right\|_{L^2(Q)}^2 &\leq \left\|\nabla u_n^k(0)\right\|_{L^2(\Omega)}^2 \\ &\leq \left\|\nabla u_0\right\|_{L^2(\Omega)}^2 \leq |\Omega| c_1(u_0)\,. \end{aligned} \tag{14}$$

Finally, relations (12), (13), and (14) yield

$$\begin{aligned} \left\|u_n^k\right\|_{H^1(Q)}^2 &\leq \left\|u_n^k\right\|_{L^2(Q)}^2 + \left\|\frac{\partial}{\partial t} u_n^k\right\|_{L^2(Q)}^2 + \left\|\nabla u_n^k\right\|_{L^2(Q)}^2 \\ &\leq |\Omega| c_1 T\left(c_2 + \frac{1}{c_0' T} + 1\right) = c_3\,, \end{aligned} \tag{15}$$

where $c_3 = c_3(C, \lambda, u_0, Q)$. Therefore, the following remark holds

Remark IV.1. *Inequality (15) means that sequence $\left\{u_n^k\right\}_{n\in\mathbb{N}}$ is uniformly bounded in $H^1(Q)$-norm independently of n and k.*

3) Passage to limit: Remark (IV.1) implies that there exists a subsequence of $\left\{u_n^k\right\}_{n\in\mathbb{N}}$ which is weakly converging in $H^1(Q)$. The subsequence is identified with $\left\{u_n^k\right\}_{n\in\mathbb{N}}$. Its limit with respect to n is denoted by u^k. From the Rellich-Kodrachov theorem, it follows that $H^1(Q)$ is compactly embedded in $L^2(Q)$; therefore, it can be seen that $u_n^k \to u^k$ in $L^2(Q)$. It remains to examine the convergence of the nonlinear terms $H_k(u_n^k)$.

To do this, it will be verified that the functions H_k are Lipschitz continuous. Considering functions w and $\hat{w}$ from $L^2(Q)$ and k fixed, auxiliary function g is defined almost everywhere on Q as a mapping from $[0,1]$ into the interval with margins $H_k(w)$ and $H_k(\hat{w})$ in the following way

$$g(\kappa) = H_k(\kappa w + (1-\kappa)\hat{w})\,.$$

Using the mean value theorem and the boundedness of the derivative of H_k (achieved by the particular form of H_k), it can be seen that

$$\begin{aligned} |H_k(w) - H_k(\hat{w})| &= |g(1) - g(0)| = |g'(\mu)| \\ &= |H_k'||w - \hat{w}| \leq c_4|w - \hat{w}| \end{aligned} \tag{16}$$

almost everywhere on Q. An arbitrary w as above is assumed. Then, inequality (16) yields

$$\begin{aligned} &\left|\left(H_k(u_n^k) - H_k(u^k), w\right)_{L^2(Q)}\right| \\ &\quad = \left|\int_Q \left[H_k(u_n^k) - H_k(u^k)\right] w \mathrm{d}\mathbf{x}\mathrm{d}t\right| \\ &\quad \le \int_Q \left|H_k(u_n^k) - H_k(u^k)\right| |w| \mathrm{d}\mathbf{x}\mathrm{d}t \\ &\quad \le c_4 \int_Q \left|u_n^k - u^k\right| |w| \mathrm{d}\mathbf{x}\mathrm{d}t \\ &\quad \le c_4 \left\|u_n^k - u^k\right\|_{L^2(Q)} \|w\|_{L^2(Q)} . \end{aligned} \tag{17}$$

Since $u_n^k \to u^k$, (17) implies that $H_k(u_n^k) \rightharpoonup H_k(u^k)$ as $n \to \infty$.

Now, using the variational formulation of problem (8)

$$\begin{aligned} 0 = &\int_Q \left(H_k(u_n^k) \frac{\partial}{\partial t} v - \lambda \nabla u_n^k \nabla v \right) \mathrm{d}\mathbf{x}\mathrm{d}t \\ &+ \int_\Omega H_k(\mathcal{P}_n u_0(\mathbf{x})) v(0, \mathbf{x}) \, \mathrm{d}\mathbf{x} , \end{aligned}$$

it is possible to pass to the weak limit with respect to n and to get

$$\begin{aligned} 0 = &\int_Q \left(H_k(u^k) \frac{\partial}{\partial t} v - \lambda \nabla u^k \nabla v \right) \mathrm{d}\mathbf{x}\mathrm{d}t \\ &+ \int_\Omega H_k(u_0(\mathbf{x})) v(0, \mathbf{x}) \, \mathrm{d}\mathbf{x} . \end{aligned}$$

Then, u^k becomes the weak solution of auxiliary problem (8).

B. Convergence of the auxiliary solutions

Remark IV.1 implies that

$$\left\|u^k\right\|^2_{H^1(Q)} \le c_3 .$$

Therefore, there exists a weakly converging subsequence of $\left\{u^k\right\}_{n\in\mathbb{N}}$ in $H^1(Q)$. Identifying it with $\left\{u^k\right\}_{n\in\mathbb{N}}$, the term

$$\begin{aligned} &\left(H_k(u^k) - H(u), w\right)_{L^2(Q)} \\ &\quad = \left(H_k(u^k) - H_k(u) + H_k(u) - H(u), w\right)_{L^2(Q)} \end{aligned}$$

tends to zero as $k \to \infty$ because $H_k(u^k) - H_k(u) \rightharpoonup 0$ by analogous process to (17) and $H_k \to H$ by the construction of $\{H_k\}_{k\in\mathbb{N}}$. Consequently, it is possible to pass to the weak limit in the variational formulation of original problem (6)

$$\begin{aligned} 0 = &\int_Q \left(H_k(u^k) \frac{\partial}{\partial t} v - \lambda \nabla u^k \nabla v \right) \mathrm{d}\mathbf{x}\mathrm{d}t \\ &+ \int_\Omega H_k(u_0(\mathbf{x})) v(0, \mathbf{x}) \, \mathrm{d}\mathbf{x} \end{aligned}$$

to obtain weak equality (7)

$$\begin{aligned} 0 = &\int_Q \left(H(u) \frac{\partial}{\partial t} v - \lambda \nabla u \nabla v \right) \mathrm{d}\mathbf{x}\mathrm{d}t \\ &+ \int_\Omega H(u_0(\mathbf{x})) v(0, \mathbf{x}) \, \mathrm{d}\mathbf{x} . \end{aligned}$$

Then, the limit u of the sequence of the auxiliary problem solutions u^k satisfies Definition III.1.

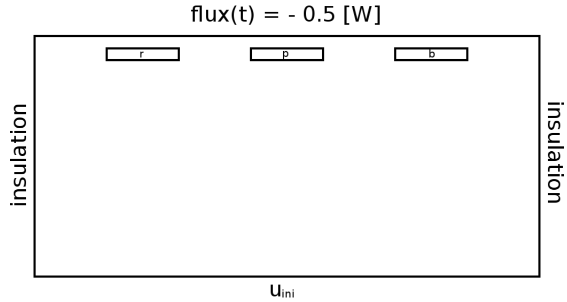

Fig. 3. The initial conditions and the thermal boundary conditions.

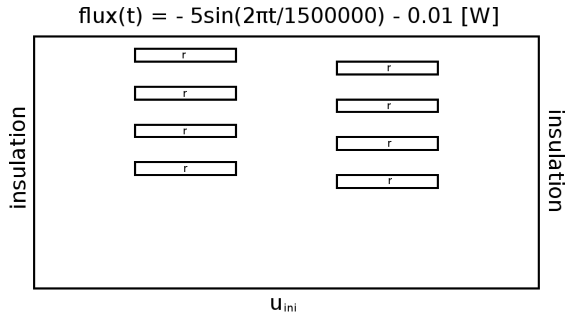

Fig. 4. The initial conditions and the thermal boundary conditions.

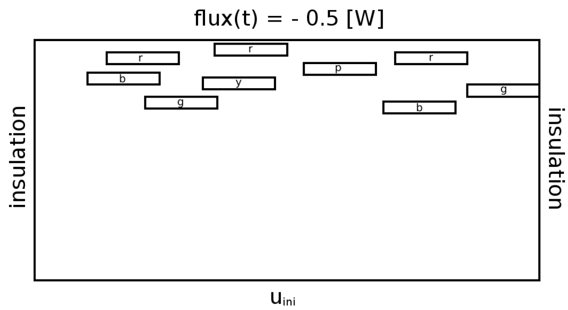

Fig. 5. The initial conditions and the thermal boundary conditions.

V. Computational Studies

Computational studies based on the model given by (1) and (3) with heterogeneities in the thermal and mechanical properties are presented in Figure 6, 7, and 8. To reduce computational constraints, the modification of the model within the meaning of employing the regularized functions ϕ and ϑ with $\varepsilon = 10^{-4}$ (see Figure 2) was applied. Considering small temperature range use and thus small potential portion ($\eta = 0.3$) of the ice fraction, all soil parameters were assumed to be constant.

The simulation settings are illustrated in Figure 3, 4, and 5, where inner rectangles denote the distribution of the property heterogeneities; the side and bottom boundaries are fixed. Different letters in the figures denote the materials of different properties, and these property differences are distinguished by adding the index to the property symbol. The values of the used parameters have rather testing than practical meaning. The scale is in meters. Figure 6 gives the qualitative comparison of the strain evolution during freezing of the soil sample with three heterogeneities. As the freezing front passes the heterogeneities, the various rate of strain response is observed depending on the type of

TABLE I
PARAMETERS OF THE MODEL (RELATED TO FIGURE 3)

Parameter	Symbol	Value	Unit
freezing point depression	$u^{\star}$	-0.1	$^{\circ}C$
initial temperature	u_0	-0.05	$^{\circ}C$
internal stress rate	χ	$5\cdot 10^7$	1
Poisson's ratio	ν, ν_r	0.33	1
Poisson's ratio	ν_b, ν_p	$8.25\cdot 10^{-2}$	1
soil density	ϱ, ϱ_r	$1.5\cdot 10^3$	$kg\cdot m^{-3}$
soil parameter	b	0.5	1
thermal conductivity	λ, λ_b	2	$W\cdot(m\cdot K)^{-1}$
thermal conductivity	λ_p, λ_r	0.1	$W\cdot(m\cdot K)^{-1}$
vol. heat capacity	C, C_b	$5\cdot 10^6$	$J\cdot(m^3\cdot K)^{-1}$
vol. heat capacity	C_p, C_r	$2.5\cdot 10^7$	$J\cdot(m^3\cdot K)^{-1}$
vol. latent heat of water	L	$3.33\cdot 10^8$	$J\cdot m^{-3}$
Young's modulus	E, E_r	$2\cdot 10^8$	Pa
Young's modulus	E_b, E_p	$5\cdot 10^7$	Pa

TABLE II
PARAMETERS OF THE MODEL (RELATED TO FIGURE 4)

Parameter	Symbol	Value	Unit
freezing point depression	$u^{\star}$	-0.05	$^{\circ}C$
initial temperature	u_0	-0.02	$^{\circ}C$
internal stress rate	χ	$7.5\cdot 10^7$	1
Poisson's ratio	ν	0.33	1
Poisson's ratio	ν_r	0.165	1
soil density	ϱ, ϱ_r	$1.75\cdot 10^3$	$kg\cdot m^{-3}$
soil parameter	b	0.4	1
thermal conductivity	λ	3	$W\cdot(m\cdot K)^{-1}$
thermal conductivity	λ_r	0.225	$W\cdot(m\cdot K)^{-1}$
vol. heat capacity	C	$4\cdot 10^6$	$J\cdot(m^3\cdot K)^{-1}$
vol. heat capacity	C_r	$1.6\cdot 10^7$	$J\cdot(m^3\cdot K)^{-1}$
vol. latent heat of water	L	$3.33\cdot 10^8$	$J\cdot m^{-3}$
Young's modulus	E	$1.8\cdot 10^8$	Pa
Young's modulus	E_r	$4.5\cdot 10^7$	Pa

heterogeneity below the observed location. On the left-hand part of the sample, a slight negative rate is even observed owing to the long relaxation time for temperature of the heterogeneity and no difference in Young's modulus of the left-hand heterogeneity and of the surrounding material.

The parameters, the initial and boundary conditions of this model are given by Table I and Figure 3.

A simulation of the development of soil freezing and thawing deformation effects is shown in Figure 7. The figure covers one period of a heat exchange and demonstrates the elastic property of soil in relation to the reverse thermal processes. The setting is similar to the previous simulation and is illustrated in Figure 4 and given by Table II.

Figure 8 represents the progress of the gradual soil freezing with its deformation effect, where the initial and thermal boundary conditions are illustrated in Figure 5. The values of the parameters used for the shown simulation are written in Table III.

VI. CONCLUSION

The presented model includes a basic heat and force balance and was designed for the purpose of the preliminary study of structural changes in saturated soils caused by the phase transition of the water content due to the

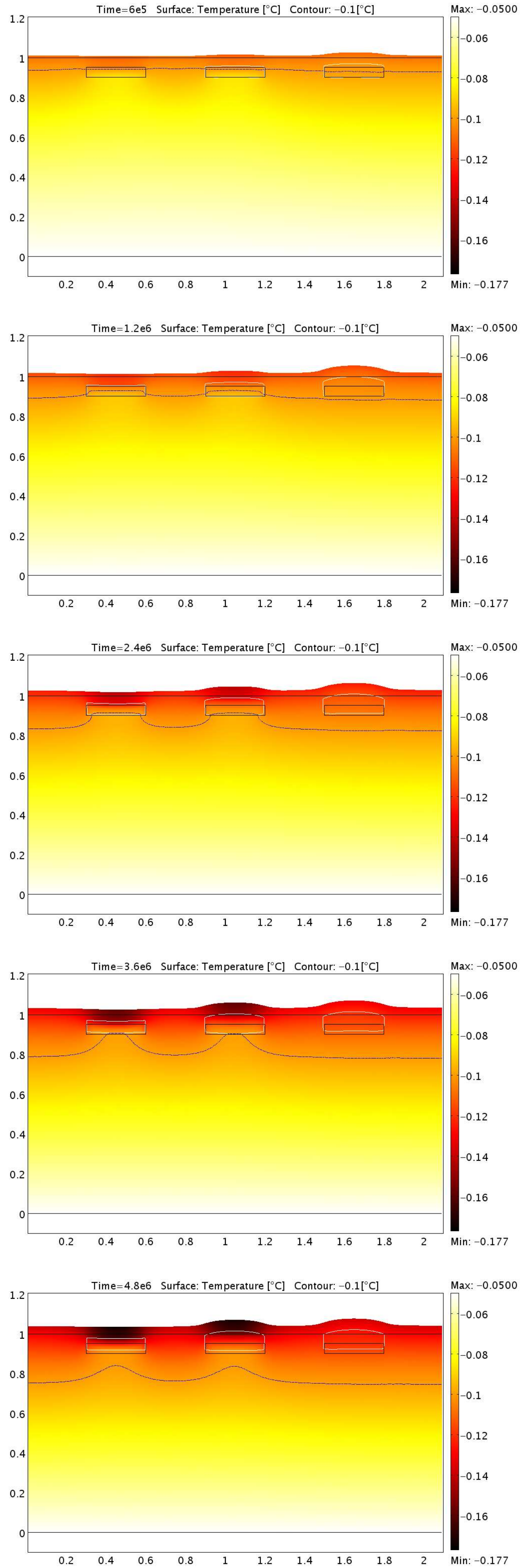

Fig. 6. Strain response rate comparison.

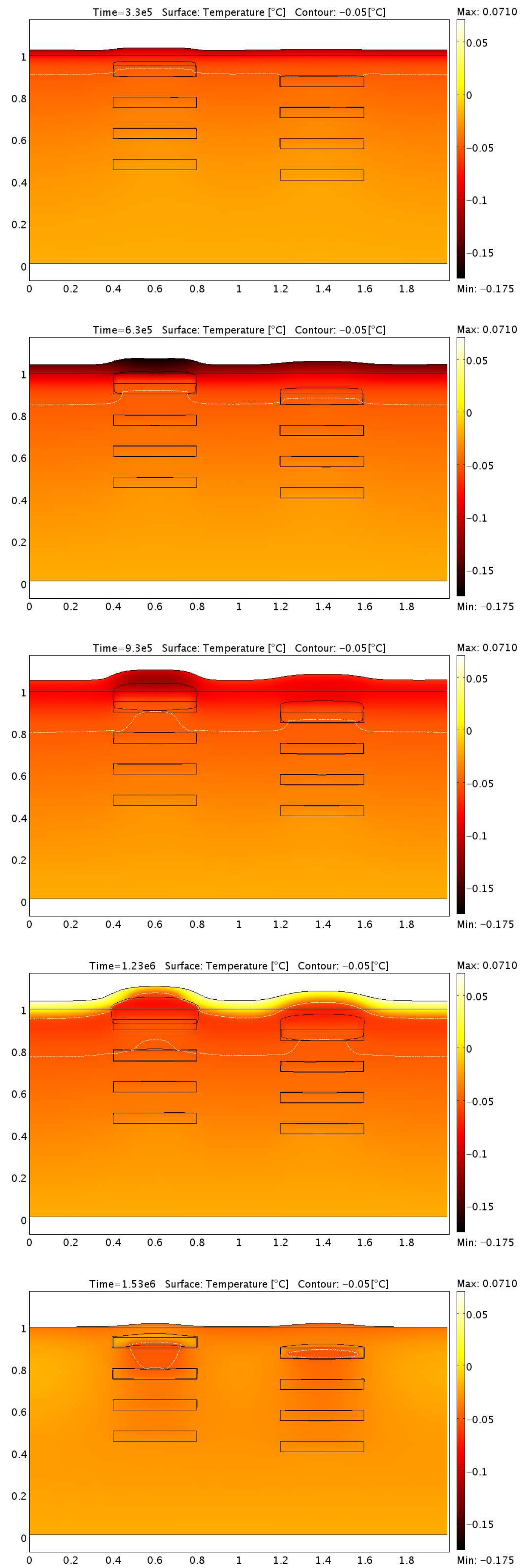

Fig. 7. Soil freezing and thawing deformation effects.

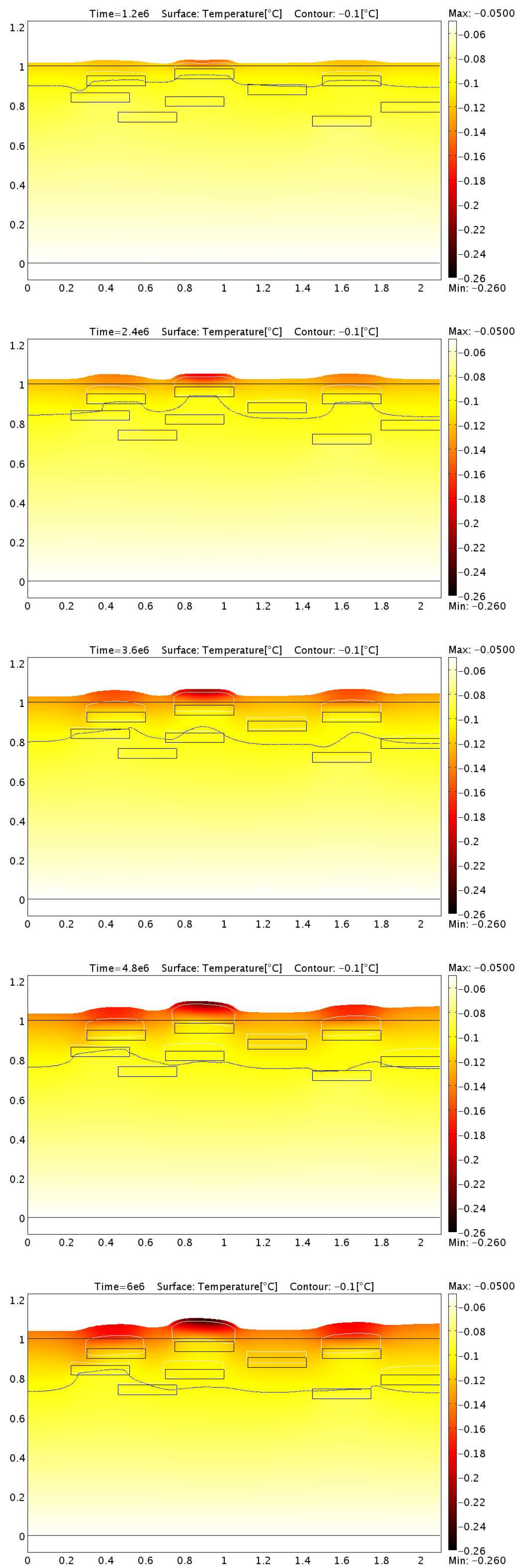

Fig. 8. Soil freezing deformation effects.

TABLE III
PARAMETERS OF THE MODEL (RELATED TO FIGURE 5)

Parameter	Symbol	Value	Unit
freezing point depression	$u^\star$	-0.1	$°C$
initial temperature	u_0	-0.05	$°C$
internal stress rate	χ	$5{\cdot}10^7$	1
Poisson's ratio	ν	0.33	1
Poisson's ratio	ν_b, ν_p	0.2475	1
Poisson's ratio	ν_g, ν_r, ν_y	0.165	1
soil density	$\varrho, \varrho_b, \varrho_r$	$1.5{\cdot}10^3$	$kg{\cdot}m^{-3}$
soil density	ϱ_p, ϱ_y	$1.8{\cdot}10^3$	$kg{\cdot}m^{-3}$
soil density	ϱ_g	$2.25{\cdot}10^3$	$kg{\cdot}m^{-3}$
soil parameter	b	0.5	1
thermal conductivity	λ, λ_g	2	$W{\cdot}(m{\cdot}K)^{-1}$
thermal conductivity	λ_b, λ_r	0.1	$W{\cdot}(m{\cdot}K)^{-1}$
thermal conductivity	λ_p, λ_y	4	$W{\cdot}(m{\cdot}K)^{-1}$
vol. heat capacity	C, C_p, C_y	$5{\cdot}10^6$	$J{\cdot}(m^3{\cdot}K)^{-1}$
vol. heat capacity	C_b, C_r	$2.5{\cdot}10^7$	$J{\cdot}(m^3{\cdot}K)^{-1}$
vol. heat capacity	C_g	$2.5{\cdot}10^6$	$J{\cdot}(m^3{\cdot}K)^{-1}$
vol. latent heat of water	L	$3.33{\cdot}10^8$	$J{\cdot}m^{-3}$
Young's modulus	E	$2{\cdot}10^8$	Pa
Young's modulus	E_b, E_p	$2.5{\cdot}10^8$	Pa
Young's modulus	E_g, E_r, E_y	$5{\cdot}10^7$	Pa

alternations of climate conditions. The thermal part of the model allowing for the phase change of the water fraction was mathematically analyzed providing the information on the weak solution existence.

Although the model is based on the continuum approach and built on simplified relations, the produced simulations reflect adequately the common empirical knowledge of the soil freezing and thawing process and the related mechanical manifestations. Further development will involve an application of more sophisticated and more descriptive relations taking laws of thermodynamics and balances of dynamic quantities into consideration. For example, the heat capacity and thermal conductivity should be also considered to be depended on the phase change.

REFERENCES

[1] S. Taber, "Frost Heaving", The Journal of Geology, Vol. 37, No. 5, pp. 428–461, Jul. - Aug. 1929.

[2] R. D. Miller, "Frost Heaving in Non-Colloidal Soils", in Proc. 3rd Int. Conference on Permafrost, pp. 707–713, 1978.

[3] R. R. Gilpin, "A Model for the Prediction of Ice Lensing and Frost Heave in Soils", Water Resources Research, Vol. 16, No. 5, pp. 918–930, 1980.

[4] K. O'Neill and R. D. Miller, "Exploration of a Rigid Ice Model of Frost Heave", Water Resources Research, Vol. 21, No. 3, pp. 281–296, 1985.

[5] A. C. Fowler, "Secondary Frost Heave in Freezing Soils", SIAM J. APPL. Math., Vol. 49, No. 4, pp. 991–1008, 1989.

[6] R. L. Michalowski, "A Constitutive Model of Saturated Soils for Frost Heave Simulations", Cold Region Science and Technology, Vol. 22, Is. 1, pp. 47–63, 1993.

[7] R. L. Michalowski and F. ASCE and M. Zhu, "Modeling and Simulation of Frost Heave Using Porosity Rate Function", Geomechanics II: Testing, Modeling, and Simulation, ASCE, pp. 178–187, 2005.

[8] K. Hansson et al., "Water Flow and Heat Transport in Frozen Soil: Numerical Solution and Freeze-Thaw applications", Vadose Zone Journal, Vol. 3, pp. 693–704, 2004.

[9] H. B. Tabrizi and F. Sadeghpour, "Solidification of Porous Material under Natural Convection by Three Phase Modeling", in Proc. of the World Congress on Engineering 2012, Vol. 3, pp. 1975–1979, 2012.

[10] A. R. Ansati et. al., "A Note on Certain Perturbation Methods for Solving the Problem of Fully Developed Flow Through a Porous Channel", IAENG International Journal of Applied Mathematics, Vol. 40, No. 4, pp. 224–232, 2010.

[11] L. H. Wiryanto, "Unsteady Waves Generated by Flow over a Porous Layer", IAENG International Journal of Applied Mathematics, Vol. 40, No. 4, pp. 233–238, 2010.

[12] Z. A. Aziz and F. Salah and D. L. Ch. Ching, "On Accelerated Flow for MHD Generalized Burgers' Fluid in a Porous Medium and Rotating Frame", IAENG International Journal of Applied Mathematics, Vol. 41, No. 3, pp. 199–205, 2011.

[13] J. Hartikainen and M. Mikkola, "Thermomechanical Model of Freezing Soil by Use of the Theory of Mixtures", in Proc. of the 6th Finnish Mechanics Days, pp. 1–6, 1997.

[14] M. Mikkola and J. Hartikainen, "Mathematical Model of Soil Freezing and Its Numerical Implementation", International Journal for Numerical Methods in Engineering, Vol. 52, pp. 543–557, 2001.

[15] N. Li et al., "Theoretical Frame of the Saturated Freezing Soil", Cold Regions Science and Technology, Vol. 35, pp. 73–80, 2002.

[16] N. Li et al., "Theoretical Modeling Framework for an Unsaturated Freezing Soil", Cold Regions Science and Technology, Vol. 54, pp. 19–35, 2008.

[17] O. Coussy, "Poromechanics of Freezing Materials", Journal of the Mechanics and Physics of Solids, Vol. 53, pp. 1689–1718, 2005.

[18] M. Aichi and T. Tokunaga, "Material Coefficients of Multiphase Thermoporoelasticity for Anisotropic Micro-hetorogenous Porous Media", International Journal of Solids and Structures, Vol. 49, pp. 3388–3396, 2012.

[19] D. J. Nicolsky, V. E. Romanovsky, G. G. Panteleev: "Estimation of soil thermal properties using in-situ temperature measurements in the active layer and permafrost", Cold Regions Science and Technology, Vol. 55, pp. 120–129, 2009.

[20] O. A. Oleinik, "One Method for Solving General Stefan Problem", Proc. of USSR Acad. of Sci., pp. 1054–1057, 1960 (in Russian).

[21] B. M. Budak and E. N. Solov'eva and A. B. Uspenskij, "Difference Method with Smoothing Factors for Solution of Stefan Problem", GVM&MF, pp. 828–840, 1965 (in Russian).

[22] A. Visintin, Models of Phase Transitions, Boston, USA: Birkäuser, 1996, ch. 5, pp. 123–152.

[23] S. L. Kamenomostskaya, "On Stefan's Problem", Math. Col. 53, pp. 489–514, 1961 (in Russian).

[24] M. Beneš, "Numerical Solution of Two-Dimensional Stefan Problem by Finite Difference Method", Acta Polytechnica, pp. 61–87, 1989 (in Czech).